

Numerical Study of Waste Gas Incineration Using Non-Premixed Swirl Burner and Burner with a Flame Holder

Masoud Darbandi, Maryam Hosseinzadeh

Department of Aerospace Engineering,
Centre of Excellence in Aerospace Systems,
Sharif University of Technology, Tehran, P.O. Box 11365-8639, Iran
darbandi@sharif.edu; hossienzadeh.maryam@yahoo.com

Gerry E. Schneider

Department of Mechanical and Mechatronics Engineering,
University of Waterloo, Waterloo, Ontario, N2L 3G1, Canada
gerry.schneider@uwaterloo.ca

Abstract– In this work, we numerically simulate the hydrocarbon-based waste gas incineration in a vertical furnace having a horizontal flame. One important issue in incineration is to keep the pollution emissions in their minimum level. Two important toxic air pollutants are CO and NO_x emissions. Evidently, unsuitable burning of the waste gases can result in such pollution emission. In this paper, we choose two burner types to investigate their effect in reducing the emission of CO pollutant from the incinerator stack. Case one is a swirl burner in which air is injected through 45 degrees swirl gaps into the incinerator. However, case two is a burner with a flame holder. Case one should provide a better rotational flow with positive impacts on the combustion efficiency. However, case two uses a flame holder, which can result in a better combustion achievement in the incinerator. We subsequently study the effects of using these two flames on the achieved temperature in the incinerator, and CO and O₂ distributions within the incinerator as well as the resulting flame shape. We show that in case one, carbon monoxide emission is less than that of case 2. In case 2, the combustion is fulfilled more completely and the achieved temperature will be sufficiently high. This is a reason for lower CO emission for Case 2. The current study also shows that case 1 results in a thinner flame shape comparing with case 2.

Keywords: Incineration, incinerator, Computational Fluid Dynamics, waste gas inlet, mixing, flame holder, Burner

1. Introduction

Burning is a primary solution to get rid of wide ranges of industrial, municipal, and hospital waste gases. Burning technology has received rapid progresses for the last 10 to 15 years. Indeed, the waste gas incineration has become such important that it can be considered as one crucial problem among serious ones in many society issues. Incinerator is considered as a furnace, in which the wastes are burned suitably. Evidently, pollution minimization has become a major topic in many modern waste gas incinerator design and constructions. If a waste gas is burned in an incinerator it can produce toxic pollutions in its surrounding environment. In other words, incinerators can come with a number of negative outputs such as ash, CO emission, and so on. Fortunately, these negative outputs can be suitably reduced by smart management of waste gas burning and the resulting combustion.

Since the type of burning is important in CO reduction, we consider two types of burners in our studying. In Case 1, we treat a swirl burner, in which the fuel is mixed with swirling air at the first stage. At the second stage, it is mixed with not only the incoming waste gas but also the secondary provided air. Having the flow swirled in the combustion chamber, it would help to have a better mixing in the combustion chamber with a great increase in the achieved combustion efficiency.

Buckley, et al. (1983) performed very extensive experiments on low velocity non-premixed flames and conducted some studies to inspect the effects of swirling on the efficiency of a combustion chamber and its resulting pollutants. They observed that the flow rotation and swirl can effectively reduce the NO_x and CO emissions and can enhance the combustion chamber efficiency.

As is known, swirling has important effects on the attained flame shape, created flame size, produced stability and generated combustion intensity. It is very normal to attribute a number to swirl to quantify its effect. It is assumed that a swirl number of $S \leq 0.4$ is treated as a low-order swirl and a swirl number of $S \geq 0.6$ is treated as a high-order swirl. Generally, swirl not only causes enhanced mixing rate in non-premixed flame, but also enhances the flame stability. In Case 1, our swirl burner has an inclination angle of 45 degrees.

Jabtan Termo-Bendalir is studies on the effect of swirl intensity and fuel mixture on combustion and flame characteristics of swirl burner in 2006. Small-non-premixed flames exhibit easier mixing in rotating burner. However in transient study of non-premixed flame, burner rotation in the beginning results in the formation of a soot wings on top of the flame cone. But as the rotation established, the orange region in the flame decreases and a bright blue flame, indicating complete mixing between fuel and air, replaces it. So rotation in this regard helps in mixing and thus enhances combustion. [2]

In the case two, the burner incorporates a fuel injection and flame holder. Combustion occurs in multistage, stage 1 mixing fuel and air that exit in flame holder and combustion isn't complete. Stage two air outlets to around the flame holder and is more complete combustion. Next stage with waste gas and secondary air is complete combustion.

2. Governing Equations

The current computational fluid dynamics analyses are performed by the numerical modelling of conservation laws for the mass, momentums, and energy equations for the mixture of various chemical species. The combustion fundamental and chemical kinetics are also taken into account in analysing the conservation laws. The flow equations are briefly introduced here. As the mass conservation, we have

$$\frac{\partial \rho}{\partial t} + \Delta \cdot (\rho \vec{v}) = S_m \quad (1)$$

Where ρ is the fluid density and v is the fluid velocity. The S_m is the mass source term. As the momentum equation, we can consider the flow through an infinitesimal element and derive the corresponding conservation laws as follows:

$$\frac{\partial (\rho v)}{\partial t} + \nabla \cdot (\rho v \vec{v}) = -\nabla p + \nabla \cdot (\vec{\tau}) + \rho \vec{g} + \vec{F} \quad (2)$$

Where p is the static pressure, $\vec{\tau}$ is the stress tensor, and $\rho \vec{g}$ and \vec{F} are the gravitational body force term and the external body force. The above equation can also be simplified to

$$\begin{aligned} \frac{\partial (\rho v_r)}{\partial t} + \frac{1}{r} \frac{\partial (r \rho v_x v_r)}{\partial x} + \frac{1}{r} \frac{\partial (r \rho v_r v_r)}{\partial r} &= -\frac{\partial P}{\partial r} + \frac{1}{r} \frac{\partial}{\partial x} [r \mu (\frac{\partial v_r}{\partial x} + \frac{\partial v_x}{\partial r})] \\ &+ \frac{1}{r} \frac{\partial}{\partial x} [r \mu (2 \frac{\partial v_r}{\partial x} - \frac{2}{3} (\Delta \cdot \vec{v})) - 2 \mu \frac{v_r}{r^2} + \frac{2}{3} \frac{\mu}{r} (\Delta \cdot \vec{v}) + \rho \frac{v_z^2}{r} + F_r \end{aligned} \quad (3)$$

Eventually, the energy equation is given as follows:

$$\frac{\partial(\rho E)}{\partial t} + \nabla \cdot (\vec{v}(\rho E + p)) = \nabla \cdot (K_{eff} \nabla T - \sum_j h_j \vec{J}_j + \overline{(\tau_{eff} \cdot \vec{v})}) + S_h \quad (4)$$

Where K_{eff} is the effective conductivity parameter and J_j is the diffusion flux of species j . The first three terms on the right-hand side of the above equation represent the energy transfer due to the species diffusions, the viscous dissipation, and the conduction phenomenon, respectively. The equation also includes the heat of chemical reaction and the other volumetric heat sources.

2. 1. Turbulence Model

The standard k - ϵ turbulence model is applied to model the turbulence part. To avoid heavy computational calculations, we just choose simple standard k - ϵ model. This model consisted of two equations including the turbulence kinetic energy, k , and the turbulent dissipation rate, ϵ . These equations can be written as

$$\frac{\partial(\rho k)}{\partial t} + \text{div}(\rho k \vec{U}) = \text{div} \left[\frac{\alpha_t}{\sigma_k} \text{grad}(k) \right] + 2\alpha_t E_{ij} \cdot E_{ij} - \rho \epsilon \quad (5)$$

$$\frac{\partial(\rho \epsilon)}{\partial t} + \text{div}(\rho \epsilon \vec{U}) = \text{div} \left[\frac{\alpha_t}{\sigma_\epsilon} \text{grad}(\epsilon) \right] + c_{1\epsilon} \frac{\epsilon}{k} 2\alpha_t E_{ij} \cdot E_{ij} - c_{2\epsilon} \rho \frac{\epsilon^2}{k} \quad (6)$$

Where G_k and G_b are the generations of turbulence kinetic energy due to the mean velocity gradient and buoyancy, respectively. Y_M is overall dissipation rate. $C_{1\epsilon}$, $C_{2\epsilon}$, and $C_{3\epsilon}$ are three constants provided from measurements. σ_k and σ_ϵ are two defined turbulent Prandtl numbers. Additionally, S_k and S_ϵ are two source terms. The constants are given as follows:

$$C_{1\epsilon} = 1.44, C_{2\epsilon} = 1.92, C_{3\epsilon} = 0.09, \sigma_k = 1.0, \sigma_\epsilon = 1.3 \quad (7)$$

2. 2. Combustion Modeling

The combustion model used in this modelling is a non-premixed one. The non-premixed model has ability to predict the sub-elements. The decomposition effect and the dependency between turbulence and chemistry is also included in the current calculations. This method is computationally very efficient because it does not need large amount of computations for each element in the transport equation.

The following mixture fractions definition is used for the species:

$$f = \frac{Z_i - Z_{i,ox}}{Z_{i,fuel} - Z_{i,ox}} \quad (8)$$

In the above equation, Z is the mass fraction, the subscript ox and $fuel$ denote the value at the oxidizer stream and the fuel stream inlets, respectively. In this calculation, the sum of all three mixture fractions are unity as follows:

$$f_{fuel} + f_{sec} + f_{ox} = 1 \quad (9)$$

The secondary mixture fraction is given by

$$f_{sec} = p_{sec} \cdot (1 - f_{fuel}) \quad (10)$$

Where p_{sec} is the normalized secondary mixture fraction. The mean mixture fraction is calculated from

$$\frac{\partial}{\partial t}(\rho \bar{f}) + \nabla \cdot (\rho \cdot \vec{v} \bar{f}) = \nabla \cdot \left(\frac{\mu_t}{\sigma_f} \nabla \bar{f} \right) + S_m + S_{user} \quad (11)$$

To obtain the mixture fraction, we solve the conservation equation for the mixture fraction variance as follows:

$$\frac{\partial}{\partial t}(\rho \overline{f'^2}) + \nabla \cdot (\rho \cdot \vec{v} \overline{f'^2}) = \nabla \cdot \left(\frac{\mu_t}{\sigma_f} \nabla \overline{f'^2} \right) + C_g \mu_t (\nabla \bar{f})^2 - C_d \rho \frac{\varepsilon}{k} \overline{f'^2} + S_{user} \quad (12)$$

Here, a supposed probability density function (PDF) of the mixture fraction is chosen as a means of modelling for the mixing issue.

2.3. Radiation Heat Transfer Modeling

We use the P-1 radiation model in our calculations. As is known, the optical thickness a_L parameter is very important for the selected radiation model. If L is treated as the diameter of incinerator, having $a_L > 1$ can be treated as the best choice to be used with the current P-1 model.

3. Incinerator Modelling

The current incinerator includes one burner incorporated from one air inlet, one fuel inlet, and eight waste gas inlets. Perpendicular to the incinerator horizontal section, there are six secondary air inlets, which are located tangentially with respect to the incinerator horizontal section. There are also twelve cooling air inlets located perpendicular to the incinerator vertical section. The incinerator height is about 8 meters and its vertical section diameter is about 3 meters. However, its horizontal section diameter is about 2 meters. The incinerator geometry is shown in Fig. 1.

As will be explained in details later, we will choose two different burners to evaluate the performance of this incinerator. The results of their simulations are presented shortly. These two burners are referred as Cases A and B in Fig. 2. Burner A has four fins having inclination angles of 45 degrees, They would provide suitable air rotations. Burner B has a V shape flame holder, whose tip is forwarded to the front. This flame holder can help to maintain a continuous smooth combustion there.

Considering the two burners given in Fig. 2, we can predict very chemical and physical behaviours occurring in the current incinerator. At the first stage of the incineration process, the fuel and air enter from their inlets located on the burner. At the next stage, the waste gas enters into the air-fuel mixture and starts burning. As the final stage, the secondary air will enter into the domain for a more effective combustion process.

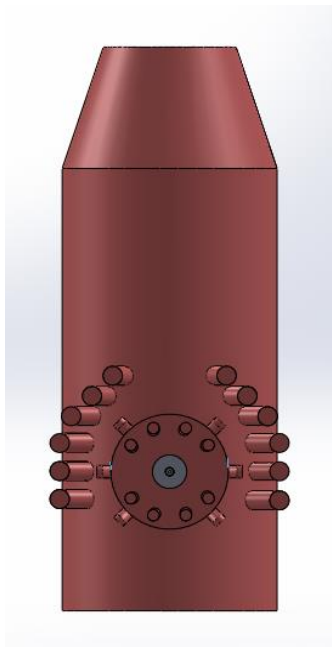


Fig. 1. The current incinerator geometry.

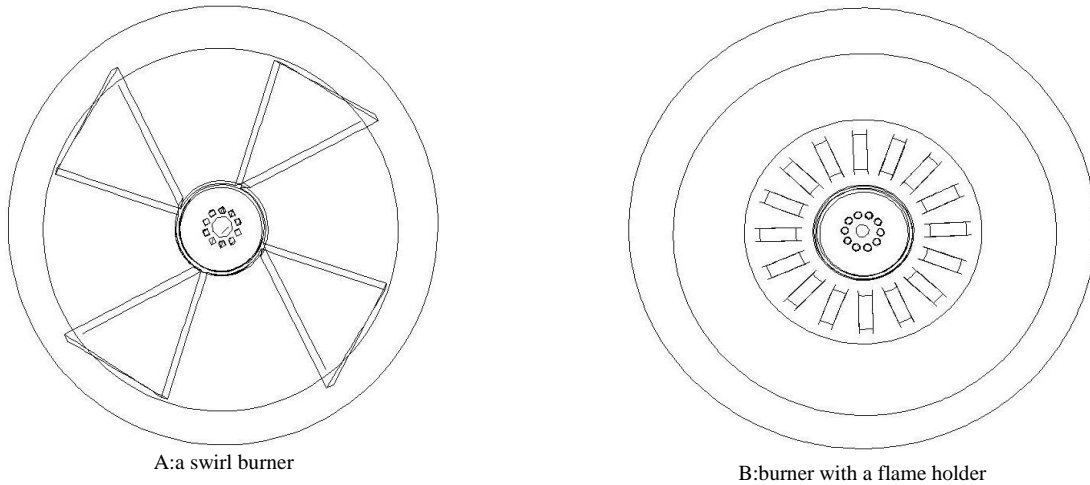


Fig. 2. Two types of burner used in this study including Case A: a swirl burner and Case B a burner with a flame holder.

We use Tet/Hybrid-Tgrid mesh to generate grids inside the incinerator. Our grid is three-dimensional with about 3,000,000 cells. We refine the grid suitably near the air, the fuel, and the waste gas inlets. We also refine the mesh suitably in the main combustion region. The heat and mass transfer calculations are suitably considered including the radiation, convection, and conduction influences inside the incinerator. We have considered different considerations in choosing the required simulation methods including the grid structure, the required boundary conditions, the flow turbulence models, and the chemical reaction models. They were briefly talked in the previous sections. As the boundary conditions, we treat the incinerator walls as adiabatic. Table 1 provide more information on the required inputs. This table says

that the combustion model is non-premixed. The fuel is methane and secondary flow consists of 38 percents nitrogen, five percents CO₂, fifteen percents O₂, and about two percents methane.

Table 1. Additional data on the inlet gases to the incinerator

Input	Mass Flow Rate	Temperature	Species
Waste Gas	3.12495 Kg/S	338 K	Pdf
Fuel	0.0277 Kg/S	313 K	Methane

4. Results and Discussion

Figure 3 presents the temperature contours inside the incinerator using Burner types 1 and 2 or A and B. Figure 3 indicate that the maximum temperature is less than 1800 K inside the incinerator. So, the two cases are under low pollution control.

Normally, we would have carbon dioxide and water vapour and nitrogen productions in many normal incinerations. However, a reduction in either the inlet air or mixing issue may cause incomplete combustion with highly toxic carbon monoxide gas production. Evidently, a suitable burner design can effectively influence the combustion efficiency and the generated species and their distributions.

Figure 4 presents the distribution of Monoxide carbon within the incinerator considering two burner types. As is seen, the maximum monoxide carbon production is about 0.181 in case 2 and 0.212 in case 1. As can be guessed, the CO does not escape from the incinerator but is fully oxidized. The combustion can occur in two stages. First, the carbon monoxide is formed. Second, the oxidation of carbon monoxide to carbon dioxide happens. According to Table 2, the CO emission in case 1 is lower than that of Case 2. In other words, the maximum CO₂ in Case 1 is more than Case 2.

Table 2. Monoxide and dioxide carbon production rates in the incinerator

Mass Fraction	Mole Fraction Of CO	Case A	Case B
CO	Mass-Weighted Average	19.71 ppm	30.95 ppm
CO	Minimum of Vertex Values	15.93 ppm	21.11 ppm
CO ₂	Mass-Weighted Average	2556.31 ppm	2433.60 ppm
CO ₂	Minimum of Vertex Values	2523.07 ppm	2399.58 ppm

We can describe the oxidation of CO assuming water as the primary hydrogen-containing species as follows:



We can conclude that the other species; such as oxygen and OH can be effective in dioxide carbon production. Figure 5 presents the O₂ and OH contours in the incinerator considering two types burners. The oxygen rates are almost identical in two investigated cases. But, different burners have caused different oxygen distributions in the incinerator. In other words, the concentration of oxygen is low in the centre of horizontal part of the furnace. It is because the combustion performs the most intensive one in this region. As is seen, this region is larger for case 1 than case 2. So, this means that the species distributions would be different in these two cases.

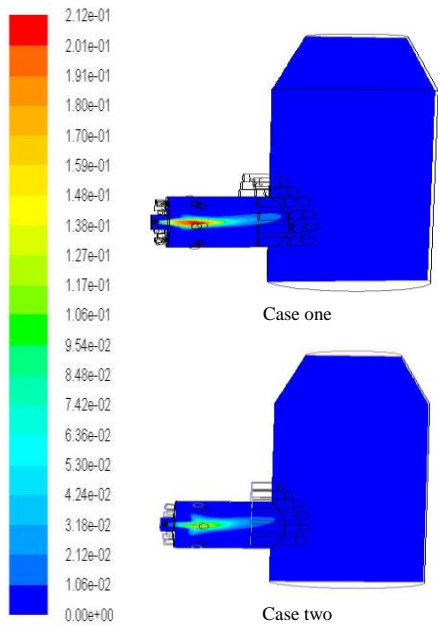


Fig. 3. The temperature contours inside the incinerator

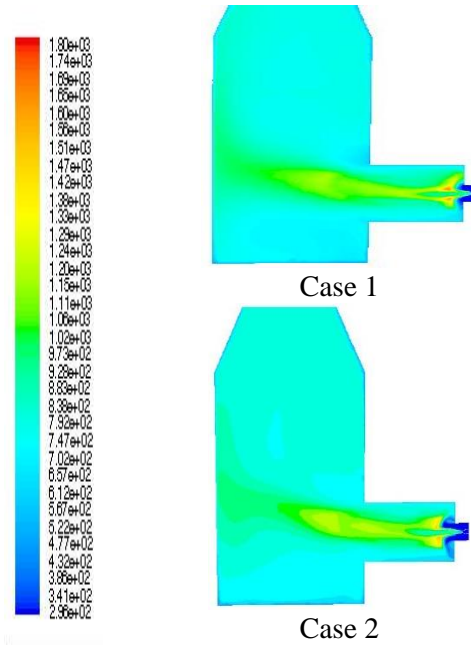


Fig. 4. The CO contours inside the incinerator

Figure 6 shows the OH species contours for the two studied cases. As is seen, the flame surface for case 2 is more than case 1. It can be attributed to high radiation effects, which cause a higher maximum temperature. So, the flue gas temperature for Case 2 is lower than Case 1.

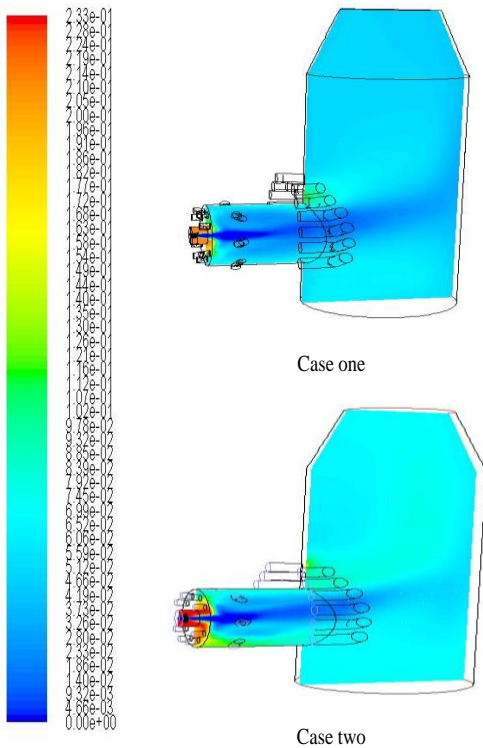


Fig. 5. The O₂ contours inside the incinerator

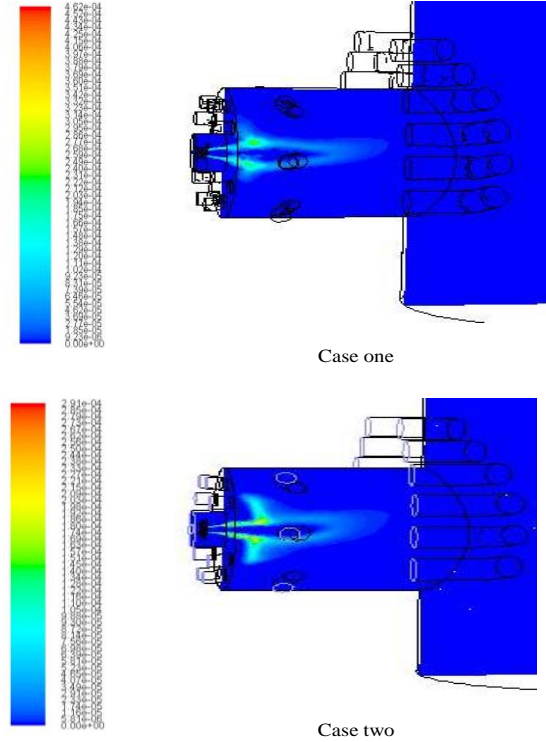


Fig. 6. The OH contours inside the incinerator

5. Conclusion

We investigated the effect of burner type in producing pollutant emission from a waste gas incinerator. The two swirl type and burner with flame holder were studied here. It was observed that the swirl type burner can provide a better stable flame. The swirled burner also provided better temperature and pollutant emissions from the incinerator. In other words, the swirled burner provides less CO emission. However, it should be reminded that a high temperature in the incinerator may promote the NO_x production, which is a negative point from the emission control.

Acknowledgements

The authors would like to thank the financial support received from the Deputy of Research and Technology in Sharif University of Technology. Their financial support and help are greatly acknowledged.

References

- Buckley, P. L., Craig, R. R., Davis, D. L., and Scharzkopf, K. G. (1983). The Design and Combustion Performance of Practical Swirlers for Integral Rocket/Ramjet, *AIAA J*, vol. 21, no. 5, pp. 740-743.
- Jabatan, T. B. Studies on the effect of swirl intensity and fuel mixtures on combustion and flame characteristics swirl burner, *Fakulti Kejuruteraan Mechanical.*, University Teknologi Malaysia, Research Vote Num: 75181.
- Ryu, C, Shin, D, and Choi, S, Bed combustion and gas flow model for MSW incinerator, *Dept. of Mech. Eng., Korea Advanced Institute of Science and Technology*, Yusong-gu, Taejon, pp. 305-701
- Surjosatyo, A., and Priambodho, Y. D. Kwok, C. K. (2011). Investigation of gas swirl burner characteristic on biomass gasification system using combustion unit equipment (CUE), *AIAA J.*, no. 33, pp. 15-33, December.

- Kerr, N. M. (1965). Swirl Effect on Flame Performance and the Modelling of the Swirling Flames, *Journal of the Institute of Fuel*, vol. 39, pp. 527-538.
- Mathur, M. L., and Maccallum, N. R. L. (1976). Swirling Air Tests Issuing from Vane Swirls, *Journal of Institute of Fuel*, vol. 41, pp. 238-24.
- Gupta, A. K., Lilley, D. G., and Syred, N. (1984). "Swirl Flows," Abacus Press, Cambridge.
- Yuasa, S., Effects of Swirl on Stability of Jet Diffusion Flames, *Combustion and Flame*, vol. 66, 1986, pp. 181-192.
- Feikema, D., Chen, R. H., and Driscoll, J. F. (1990). Enhancement of Blowout Limits by the Use of Swirl, *Combustion and Flame*, vol. 80, pp. 183-195.
- Zengying, L., and Xiaoqian, MA. (2010). Mathematical modeling of MSW combustion and SNCR in a full-scale municipal incinerator and effects of grate speed and oxygen-enriched atmospheres on operating conditions, *Waste Management*, vol. 30, pp. 2520–2529.
- Giuseppe, L., Nicola, V., and Marco, B. (2010). The benefits of flue gas recirculation in waste incineration, *Waste Management*, vol. 27, 2007, pp. 106–116.